

Simulation and optimization of sensor based on Mach-Zehnder interferometer with reference waveguide

M. KUSKO

National Institute for Research and Development in Microtechnologies, IMT-Bucharest, Romania

This work presents the theoretical results regarding the optimization of an integrated Mach-Zehnder interferometer with a calibration waveguide refractometer based on silicon nitride rib waveguides with SU8 cladding. From modeling and simulation studies a sensor structure has been designed which presents toleration to fabrication errors and input coupling misalignments. The role of the chromium thin layer sections deposited over silicon nitride layer is analyzed in this work for alleviating the misalignment coupling errors and for improvement of the measurement accuracy, respectively.

(Received January 24, 2013; accepted November 7, 2013)

Keywords: Sensing, Simulations, Photonic integrated circuits

1. Introduction

The integrated Mach-Zehnder interferometer (MZI) is one of the most studied type of label-free evanescent wave immunosensor due to the high level of the sensitivity which can be achieved via interferometric measurements [1]. Essentially, a classical integrated MZI consists in an input waveguide, followed by a Y junction which equally divides the input radiation on two arms (waveguides): the reference waveguide and the sensing waveguide. The latter waveguide has a window which permits the interaction of the waveguide's evanescent wave with the surrounding medium. The radiation propagating on two arms is recombined via another Y-junction in the output waveguide. The alteration of the phase radiation due to the evanescent wave interaction with the bulk analyte and/or the adsorbed layers influences the intensity in the output waveguide due to the interference of radiation between the reference and sensing waveguide. Even if the study of the first sensors based on integrated MZI have begun twenty years ago [2], there are a lot of technical drawbacks which hampers the use of MZI in commercial sensors especially for sensors dedicated to work for to point of care applications. The MZI shortcomings are related to the periodic nature of the sensor response, the need for the precise alignment of the launching radiation fibre with the input waveguide and the source power fluctuations which can alter the accuracy of the sensor response. Both the precise alignment and source power stability conditions are caused by the direct recording of the output signal.

The use of a reference waveguide which allows the simultaneous measurement of the sensor signal and a reference signal represents a method to circumvent this problem [3-5]. In this work a classical MZI with a reference waveguide is theoretically analysed by considering the factors that may affect the measurement accuracy and the modalities to minimise and even eliminate their influence. The MZI discussed here is composed of a Y-junction which divides the incoming

radiation in the reference waveguide and the proper MZI. The radiation emitted at the exit of the reference waveguide and the exit of the MZI's output waveguide, respectively, may be collected via a microscope objective on a CCD matrix or on two photodiodes, the ratio between MZI output signal and reference waveguide signal rendering the true response of the MZI sensor without the influence of the coupling misalignments or the fluctuation of the radiation power source.

An important issue considered here is the design of a sensor having monotonic, linear response in a certain range of the analyte refractive indexes. Another goal of this study is to design a sensor which proves a fair tolerance to fabrications errors and coupling misalignments.

2. Design

The waveguide configuration considered in this study relies on silicon nitride ($n = 2.02$) layer on silicon dioxide substrate ($n = 1.46$). The silicon nitride layer would be very shallowly etched over a few nm in order to define a single-mode rib waveguide. SU8 polymer has been considered as the cladding material due to the capability to be processed via standard lithography and due to the negative thermo-optic coefficient which is close to the thermo-optic coefficient of the liquid analyte. The same trend for the thermo-optic coefficient of the cladding material and the analyte will minimize the errors induced by temperature variation. SU8 refractive index is considered to be 1.61. The use of polymeric materials for MZI waveguides has been reported before, either as material for waveguides [6, 7] or as support for the microfluidic circuits in the MZI sensors [8]. The radiation wavelength is 635 nm. The schematic diagram of the MZI with reference waveguide is presented in Fig. 1.

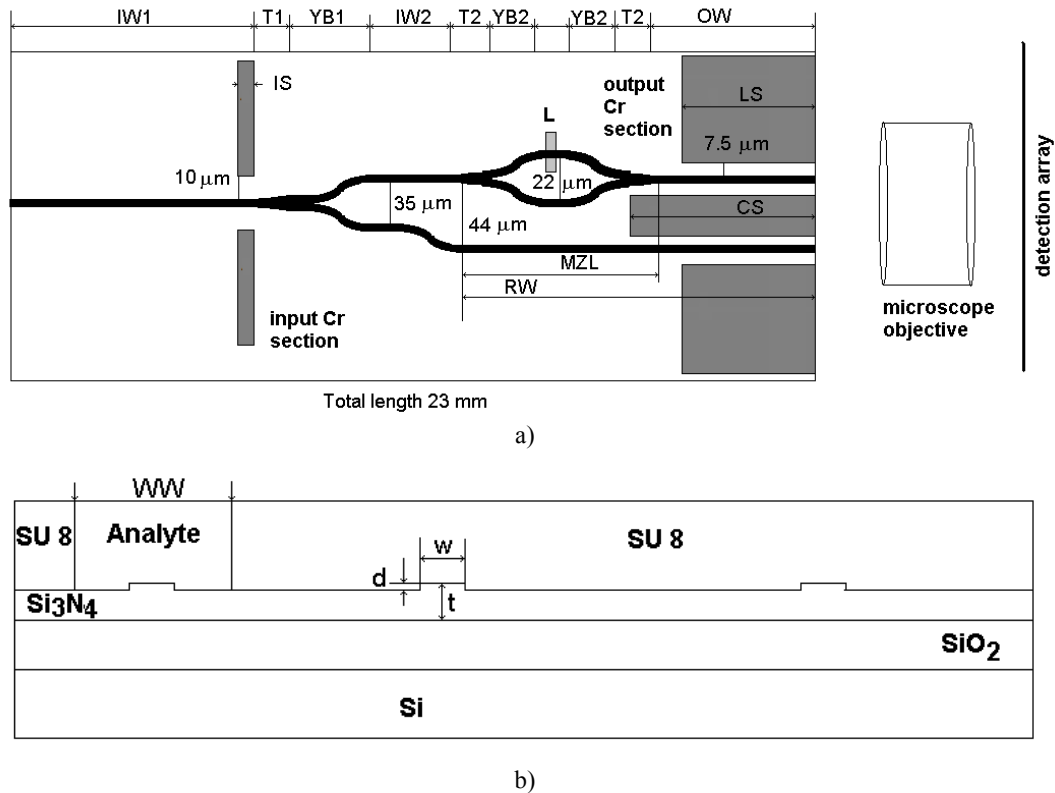


Fig. 1. The schematic diagram of the MZI sensor with reference waveguide. Top view;
b) Cross section view in the sensing window region.

The dimensions of the geometrical parameters from the Fig. 1a are listed in the following:

- Input waveguide length IW 6 mm;
- Length of the tapered section for the first branch T1 1 mm;
- Length of the first Y branch YB1 2 mm;
- Length of the input waveguide before the proper Mach-Zehnder interferometer IW2 2 mm;
- MZI length 5 mm;
- Length of the output waveguide OW 7 mm;
- Length of the tapered section for the MZI branch T2 1 mm;
- Length of the Y branch of Mach-Zehnder interferometer YB2 1.2 mm;
- MZI arm length 0.6 mm.
- Length of the reference waveguide 12 RW mm.
- Input Cr section length IS 0.1 mm.
- Central output Cr section CS 8 mm.
- Lateral output Cr section LS 3 mm.

The distance between waveguides and the distance between waveguides and Cr sections are considered to begin from the centre of the waveguides.

In the Fig. 1b w means the waveguide width, t is the waveguide thickness and d represents the depth of the rib waveguide. The window width noted as WW is 20 μm .

The configuration studied here considers more sections of a Cr layer deposited between the silicon nitride layer and the SU8 cladding. Since the deposition and configuration of the Cr sections can be done in a single step, the input Cr sections and the output Cr sections have distinctive roles. The input Cr sections help the improvement of the symmetrical coupling of radiation in the reference waveguide and the proper MZI by blocking the scattered field resulted from the coupling misalignment to the input waveguide. The output Cr sections have the role to eliminate the influence of the parasitic radiation scattered from the proper MZI, especially at destructive interference which may affect the measurement accuracy. The Cr layer thickness is 5 nm.

The beneficial role of the output Cr thin film sections for elimination of the influence of the parasitic output scattered radiation is emphasized in Fig. 2. The output scattered radiation appears at destructive interference and it may induce crosstalk between the sensing signal and the calibration signal.

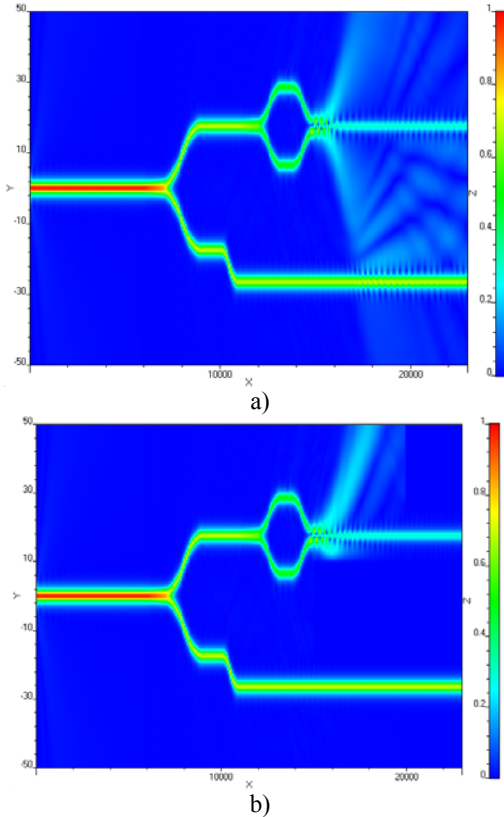


Fig. 2. The influence of the output Cr section over the radiation propagation in the sensor: a) without output Cr thin film sections; b) with output Cr thin film sections.

The reference waveguide has been placed apart from the MZI in order to eliminate the influence of the evanescent field of the reference waveguide over the proper MZI response.

The radiation propagation in the sensor has been simulated with Beam Propagation Method using OptiBPM software [9]. As a consequence of the large dimensions of the interferometer the simulations were only two-dimensional by employing the effective index method. The 2D mode solver associated with Optigrating software [9] has been used to compute the effective index for Cr sections due to the existence of a large complex part of the index of refraction.

The design of the geometric parameters of the single-mode waveguide has been performed using the free CAMFR 1.1 software. Although this software can be used only for the analysis of 2D configurations, it can be used for mode analysis of 3D waveguides with the use of the well known effective index method [10]. There are two considerations when a single-mode waveguide is designed using the effective index method. The first one requires the fulfilment of the single conditions on the vertical direction by adjusting the thickness of the silicon nitride layer. The second one imposes the single-mode condition on the lateral direction. The latter condition can be obtained by controlling both the waveguide width and the etching depth outside the waveguide, i.e. the rib height. The width

of the waveguide is set at two microns, which is accessible by standard photolithography. The value of the rib height is usually a few nanometers and may be affected by the fabrication errors. The increase of the maximum allowed rib height is directly related to the increase of the waveguide thickness. However, a compromise should be made so that one can have acceptable rib height tolerance and in the same time the single-mode operation on the vertical direction. The waveguide thickness is set at 250 nm so that the vertical single-mode condition is accomplished even if the refractive index of the analyte has the lowest value ($n = 1.33$). The rib height is 5 nm and the tolerance is ± 2 nm. Radiation polarization is TE.

The periodic nature of the output signal characteristic to the Mach-Zehnder interferometer sensor requires a careful design in order to obtain a monotonic and quasi-linear response over a certain range of the refractive index values as presented in [11]. The expected response of the MZI can be obtained by choosing the appropriate value of the window length. This parameter determines the output intensity as one can easily see from the well known equation of the Mach-Zehnder interferometer

$$I = \frac{1}{2}(1 + \cos \Delta\varphi) \quad (1)$$

where

$$\Delta\varphi = \frac{2\pi}{\lambda} L(n_{\text{effr}} - n_{\text{effs}}) \quad (2)$$

$\Delta\varphi$ expresses the phase difference between the radiation propagating in the sensing arm and the reference arm, respectively. Here L stands for the window length, while n_{effr} and n_{effs} correspond for the effective index of the reference arm and also for the effective index of the sensing arm, respectively. If $\Delta\varphi = m\pi$ (with m an odd number) then the output intensity is equal to zero and if $\Delta\varphi = m\pi$ (with m an even number) then the output intensity is 1 (the input intensity is also considered to be 1). If we consider the case when the output intensity varies from 0 to 1 in the measurement range (or vice versa), the window length should satisfy simultaneously two conditions as described in [12]:

$$\frac{2\pi}{\lambda} L(n_{\text{effr}} - n_{\text{effm}}) = m\pi \quad (3)$$

and

$$\frac{2\pi}{\lambda} L(n_{\text{effr}} - n_{\text{effM}}) = (m-1)\pi \quad (4)$$

It should be noted that it is very difficult to adjust the window length so that the conditions (3) and (4) are fulfilled at the same moment. Here, n_{effm} is the value of the sensing arm effective index corresponding to the minimal value of the analyte refractive index and n_{effM} is the sensing arm effective index associated with the maximum value of the analyte refractive index. More, due to the cosine function, the sensor response will be far from the linearity. Due to these reasons it is recommended to choose a value for the window length that satisfies the set of conditions:

$$\frac{m\lambda}{2(n_{\text{effr}} - n_{\text{effm}})} < L < \frac{(m-1)\lambda}{2(n_{\text{effr}} - n_{\text{effM}})} \quad (5)$$

The above conditions expresses that the real window length must be larger than the length associated with eq. (3) and also impose that the window length should be smaller than the length associated with eq. (4). In this analysis $n_{\text{effr}} = 1,86859$, $n_{\text{effm}} = 1,853098$ and $n_{\text{effM}} = 1,854266$. Here, n_{effm} corresponds to refractive index 1.33 and n_{effM} corresponds to refractive index 1.36.

In the Table 1 the minimal and maximum approximated values of the window length are listed for $m \geq 1$.

Table 1. The minimal and maximal values of the window length as a function of m .

m	L according to eq. (3) (μm)	L according to eq. (4) (μm)
1	20.5	0
2	41	22
3	61.5	44.5
4	82	66.5
5	102.5	88.5
6	123	111
7	143.5	133
8	164	155
9	184.5	177.5
10	205	199.5
11	225.5	221.5

If the average value of the window length between L from (3) and L from (4) is used in eq. (1) one can find that the optimal value of the window length is $138 \mu\text{m}$ in order to find a quasi-linear and also a strong response of the output intensity with the variation of the analyte refractive index in the desired refractive index measurement range (1.33 – 1.36).

4. Results

The simulations studies had the role to optimize the proposed configuration so that there would be a close resemblance between the results predicted from analytical expressions and the results obtained from the simulations. Another target of the simulations studies is the improvement of the sensor response to the input coupling misalignment.

The influence of the fabrication errors has been considered in simulations. In order to obtain close results between the theory and simulations for very shallow rib height the reference waveguide has been placed apart from the proper MZI at $44 \mu\text{m}$ so that the evanescent field of the waveguide mode (very large for small rib height) would not interact with the field propagating in the proper MZI.

The simulated sensor response has been computed from the ratio between the square of the maximum

amplitude corresponding to the MZI interferometer and the reference waveguide respectively. The variation of the sensor response as a result of the radiation input coupling misalignments may be reduced by prolonging the single-mode waveguide input section and/or by imposing a filter gate made of Cr thin film sections (see Fig. 1) which may block the scattered input field to asymmetrically excite the calibration waveguide or the proper MZI. As the length of the input waveguide cannot be increased too much, especially for a long device as the MZI with calibration waveguide, the use of an additional filter gate may be the solution of choice for the improvement of the variation of the sensor response to coupling misalignments. From simulations it appeared that the use of Cr thin film gate with $20 \mu\text{m}$ width and a input waveguide 6 mm long will bring the standard deviation below 1 percent. The standard deviation has been calculated by considering $0 \mu\text{m}$ and $\pm 0.5 \mu\text{m}$ lateral misalignments. The standard deviation calculated for the rib height of 3, 5 and 7 nm, respectively, are shown in Fig. 2a. In order to underline the beneficial role of the use of the reference waveguide with Cr thin film gate the results of the standard deviation are computed without normalizing the MZI output by the calibration waveguide output. The results are presented in Fig. 2b. One can easily notice from the comparison between the results shown in the Fig. 2a and the results presented in Fig. 2b that the use of the reference waveguide with a Cr thin film gate brings a significant improvement on the effect of the input coupling misalignments.

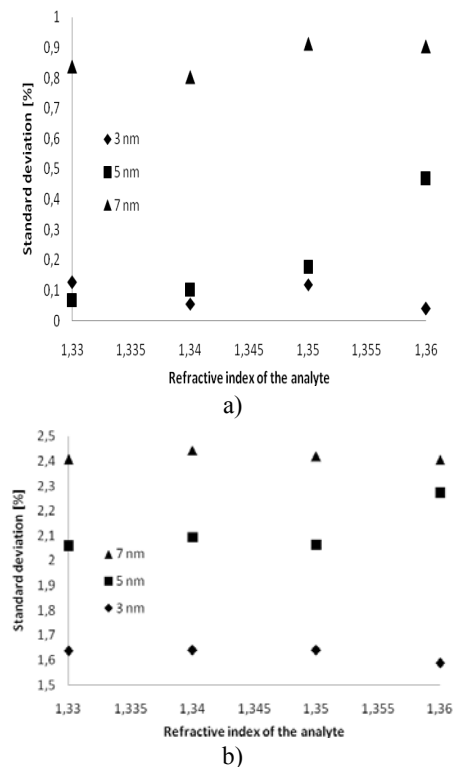


Fig. 2. The standard deviation of the sensor. a) with reference waveguide; b) without the reference waveguide.

The comparison from the theoretical results obtained for 5 nm rib height and the simulation results for the rib height of 3, 5 and 7 nm, respectively is presented in Fig. 3.

The simulations results have been obtained as an average from the sensor response corresponding to 0 μm and $\pm 0.5 \mu\text{m}$ lateral misalignments. The results obtained from simulations shows a very good agreement with the results predicted from the theory.

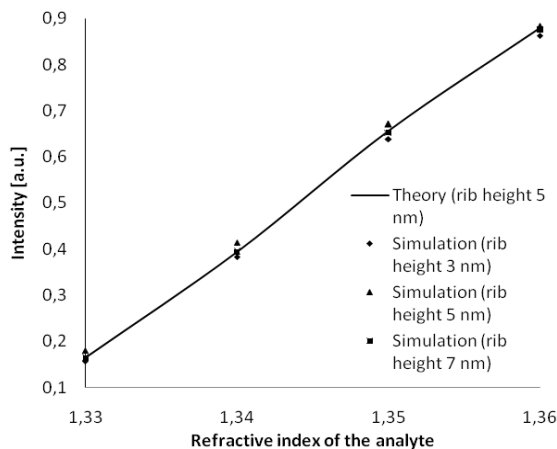


Fig. 3. Comparison between the analytical results and the results obtained from BPM simulations.

5. Conclusions

A refractometric sensor based on an integrated Mach-Zehnder interferometer with reference waveguide has been designed and simulated using BPM software in order to optimise this type of sensor.

The silicon nitride rib waveguides have been optimized to present single-mode behaviour even for fair fabrication tolerances. The length of the sensing window has been selected with the use of the analytical expressions so that one can obtain a monotonic and more preferable a quasi-linear dependence. The theoretical predicted sensor response has been confirmed by numerical simulations even if the fabrication errors have been considered.

The role of input and output Cr thin film sections for the improvement of the sensor performances has been also investigated. It has been obtained a strong attenuation of the effects associated with radiation input coupling misalignment if input Cr thin film blocking zones have been used in conjunction with the consideration of a reasonably long input waveguide. Also, the use of output Cr thin film sections may block the output scattered radiation (especially at destructive interference) so that one can avoid the crosstalk between the sensing signal and the calibration signal.

Based on the results exposed in this work one can fabricate a refractometric sensor or an immunosensor with possible point of care applications presenting good working characteristics and also good tolerances to fabrication and operating errors.

Acknowledgement

The research presented in this paper is supported by Sectoral Operational Programme Human Resources Development (SOP HRD), financed from the European Social Fund and by the Romanian Government under the contract number POSDRU/89/1.5/S/63700.

References

- [1] X. Fan, I. M. White, S. I. Shopoua, H. Zhu, J. D. Suter, Y. Sun, *Anal. Chim. Acta*, **620**, 8, (2008).
- [2] G. Heideman, R. P. H. Kooyman, J. Greve, *Sensors and Actuators B*, **10**, 209 (1993).
- [3] F. Brosinger, H. Freimuth, M. Lacher, W. Ehrfeld, E. Gedig, A. Katerkamp, F. Spener, K. Cammann, *Sensors and Actuators B: Chemical*, **44**, 350 (1997).
- [4] S. Busse, J. Käshammer, S. Krämer, S. Mittler, *Sensors and Actuators B: Chemical*, **60**, 148 (1999).
- [5] S. Busse, M. DePaoli, G. Wenz, S. Mittler, *Sensors and Actuators B: Chemical*, **80**, 116 (2001).
- [6] B. Y. Shew, Y. C. Cheng, Y. H. Tsai, *Sens. Actuators A Phys.* **141**, 299 (2008).
- [7] R. Bruck, E. Melnik, P. Muellner, R. Hainberger, M. Lammerhofer, *Biosensors and Bioelectronics* **26**, 9 3832 (2011).
- [8] B. Sepulveda, J. Sanchez del Rio, M. Moreno F. J. Blanco, K. Mayora, C. Dominguez, L. M. Lechuga, *J. Opt. A: Pure Appl. Opt.* **8**, 561 (2006).
- [9] www.optiwave.com
- [10] H. Nishihara, M. Haruna, T. Suhara, *Optical Integrated Circuits*, (New York, McGraw-Hill, 1989), pp. 31.
- [11] G. Calo, A. Farinola, V. Petruzzelli, *Progress In Electromagnetics Research Letters* **33**, 151 (2012).
- [12] M. R. Ionita, M. Kusko, *CAS 2010 Proceedings*, Sinaia, Romania, 2010, 529.

*Corresponding author: mihai.kusko@imt.ro